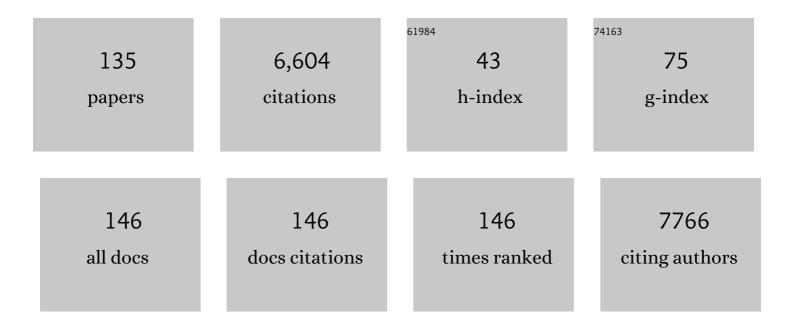
## **Jianling Zhang**

List of Publications by Year in descending order

Source: https://exaly.com/author-pdf/3663923/publications.pdf Version: 2024-02-01



#	Article	IF	CITATIONS
1	Microemulsions with ionic liquid polar domains. Physical Chemistry Chemical Physics, 2004, 6, 2914.	2.8	332
2	Metal–Organic Framework Nanospheres with Wellâ€Ordered Mesopores Synthesized in an Ionic Liquid/CO <sub>2</sub> /Surfactant System. Angewandte Chemie - International Edition, 2011, 50, 636-639.	13.8	280
3	Highly Electrocatalytic Ethylene Production from CO <sub>2</sub> on Nanodefective Cu Nanosheets. Journal of the American Chemical Society, 2020, 142, 13606-13613.	13.7	260
4	Manganese acting as a high-performance heterogeneous electrocatalyst in carbon dioxide reduction. Nature Communications, 2019, 10, 2980.	12.8	235
5	Sonochemical Formation of Single-Crystalline Gold Nanobelts. Angewandte Chemie - International Edition, 2006, 45, 1116-1119.	13.8	226
6	Highly efficient electrochemical reduction of CO <sub>2</sub> to CH <sub>4</sub> in an ionic liquid using a metal–organic framework cathode. Chemical Science, 2016, 7, 266-273.	7.4	225
7	Highly Efficient Electroreduction of CO <sub>2</sub> to Methanol on Palladium–Copper Bimetallic Aerogels. Angewandte Chemie - International Edition, 2018, 57, 14149-14153.	13.8	222
8	Efficient SO2 absorption by renewable choline chloride–glycerol deep eutectic solvents. Green Chemistry, 2013, 15, 2261.	9.0	215
9	Highly mesoporous metal–organic framework assembled in a switchable solvent. Nature Communications, 2014, 5, 4465.	12.8	177
10	MIL-125-NH <sub>2</sub> @TiO <sub>2</sub> Core–Shell Particles Produced by a Post-Solvothermal Route for High-Performance Photocatalytic H <sub>2</sub> Production. ACS Applied Materials & Interfaces, 2018, 10, 16418-16423.	8.0	143
11	Surfactant-directed assembly of mesoporous metal–organic framework nanoplates in ionic liquids. Chemical Communications, 2012, 48, 8688.	4.1	120
12	lonic liquid accelerates the crystallization of Zr-based metal–organic frameworks. Nature Communications, 2017, 8, 175.	12.8	111
13	Ru nanoparticles immobilized on metal–organic framework nanorods by supercritical CO2-methanol solution: highly efficient catalyst. Green Chemistry, 2011, 13, 2078.	9.0	108
14	Photocatalytic CO <sub>2</sub> Transformation to CH <sub>4</sub> by Ag/Pd Bimetals Supported on N-Doped TiO <sub>2</sub> Nanosheet. ACS Applied Materials & Interfaces, 2018, 10, 24516-24522.	8.0	99
15	Solvent determines the formation and properties of metal–organic frameworks. RSC Advances, 2015, 5, 37691-37696.	3.6	95
16	In situ dual doping for constructing efficient CO2-to-methanol electrocatalysts. Nature Communications, 2022, 13, 1965.	12.8	84
17	Fabrication and characterization of magnetic carbon nanotube composites. Journal of Materials Chemistry, 2005, 15, 4497.	6.7	81
18	Recovery of Silver Nanoparticles Synthesized in AOT/C12E4 Mixed Reverse Micelles by Antisolvent CO2. Chemistry - A European Journal, 2002, 8, 3879-3883.	3.3	80

#	Article	IF	CITATIONS
19	High-internal-phase emulsions stabilized by metal-organic frameworks and derivation of ultralight metal-organic aerogels. Scientific Reports, 2016, 6, 21401.	3.3	78
20	Solubility of Ls-36 and Ls-45 Surfactants in Supercritical CO2and Loading Water in the CO2/Water/Surfactant Systems. Langmuir, 2002, 18, 3086-3089.	3.5	76
21	Supercritical or Compressed CO <sub>2</sub> as a Stimulus for Tuning Surfactant Aggregations. Accounts of Chemical Research, 2013, 46, 425-433.	15.6	76
22	One-step synthesis of ultrathin α-Co(OH) <sub>2</sub> nanomeshes and their high electrocatalytic activity toward the oxygen evolution reaction. Chemical Communications, 2018, 54, 4045-4048.	4.1	71
23	Synthesis and characterization of TiO2–montmorillonite nanocomposites and their application for removal of methylene blue. Journal of Materials Chemistry, 2006, 16, 579-584.	6.7	70
24	BiOCl nanosheets with periodic nanochannels for high-efficiency photooxidation. Nano Energy, 2020, 78, 105340.	16.0	70
25	Fabrication of 2D metal–organic framework nanosheets with tailorable thickness using bio-based surfactants and their application in catalysis. Green Chemistry, 2019, 21, 54-58.	9.0	66
26	Highly efficient hydrogenation of levulinic acid into 2-methyltetrahydrofuran over Ni–Cu/Al <sub>2</sub> O <sub>3</sub> –ZrO <sub>2</sub> bifunctional catalysts. Green Chemistry, 2019, 21, 606-613.	9.0	66
27	Seleniumâ€Ðoped Hierarchically Porous Carbon Nanosheets as an Efficient Metalâ€Free Electrocatalyst for CO <sub>2</sub> Reduction. Advanced Functional Materials, 2020, 30, 1906194.	14.9	66
28	Nonaqueous microemulsion-containing ionic liquid [bmim][PF6] as polar microenvironment. Colloid and Polymer Science, 2005, 283, 1371-1375.	2.1	65
29	A Novel Method to Immobilize Ru Nanoparticles on SBA-15 Firmly by Ionic Liquid and Hydrogenation of Arene. Catalysis Letters, 2005, 103, 59-62.	2.6	63
30	Multi-shelled CuO microboxes for carbon dioxide reduction to ethylene. Nano Research, 2020, 13, 768-774.	10.4	60
31	Supramolecular Assemblies of Amphiphilic <scp>L</scp> â€Proline Regulated by Compressed CO <sub>2</sub> as a Recyclable Organocatalyst for the Asymmetric Aldol Reaction. Angewandte Chemie - International Edition, 2013, 52, 7761-7765.	13.8	58
32	Large-pore mesoporous Mn3O4 crystals derived from metal–organic frameworks. Chemical Communications, 2013, 49, 11695.	4.1	56
33	Nanoemulsions Induced by Compressed Gases. Angewandte Chemie - International Edition, 2008, 47, 3012-3015.	13.8	55
34	CO2 controls the oriented growth of metal-organic framework with highly accessible active sites. Nature Communications, 2020, 11, 1431.	12.8	51
35	A new method to recover the nanoparticles from reverse micelles: recovery of ZnS nanoparticles synthesized in reverse micelles by compressed CO2. Chemical Communications, 2001, , 2724-2725.	4.1	50
36	Hollow metal–organic framework polyhedra synthesized by a CO2–ionic liquid interfacial templating route. Journal of Colloid and Interface Science, 2014, 416, 198-204.	9.4	50

#	Article	IF	CITATIONS
37	Assembling Metal–Organic Frameworks in Ionic Liquids and Supercritical CO <sub>2</sub> . Chemistry - an Asian Journal, 2016, 11, 2610-2619.	3.3	49
38	Cellular graphene aerogel combines ultralow weight and high mechanical strength: A highly efficient reactor for catalytic hydrogenation. Scientific Reports, 2016, 6, 25830.	3.3	49
39	Fire-resistant, ultralight, superelastic and thermally insulated polybenzazole aerogels. Journal of Materials Chemistry A, 2018, 6, 20769-20777.	10.3	49
40	Micellization of long-chain ionic liquids in deep eutectic solvents. Soft Matter, 2016, 12, 5297-5303.	2.7	47
41	Pickering emulsions stabilized by a metal–organic framework (MOF) and graphene oxide (GO) for producing MOF/GO composites. Soft Matter, 2017, 13, 7365-7370.	2.7	46
42	Poly(ethylene glycol) Stabilized Mesoporous Metal–Organic Framework Nanocrystals: Efficient and Durable Catalysts for the Oxidation of Benzyl Alcohol. ChemPhysChem, 2014, 15, 85-89.	2.1	44
43	Anchoring Ionic Liquid in Copper Electrocatalyst for Improving CO <sub>2</sub> Conversion to Ethylene. Angewandte Chemie - International Edition, 2022, 61, .	13.8	44
44	Incorporation of metal-organic framework in polymer membrane enhances vanadium flow battery performance. Electrochimica Acta, 2017, 257, 243-249.	5.2	43
45	Carbon Dioxide in Ionic Liquid Microemulsions. Angewandte Chemie - International Edition, 2011, 50, 9911-9915.	13.8	42
46	Bipyridyl-Containing Cadmium–Organic Frameworks for Efficient Photocatalytic Oxidation of Benzylamine. ACS Applied Materials & Interfaces, 2019, 11, 30953-30958.	8.0	42
47	CO2 capture by hydrocarbonsurfactant liquids. Chemical Communications, 2011, 47, 1033-1035.	4.1	41
48	Nitrogen-carbon layer coated nickel nanoparticles for efficient electrocatalytic reduction of carbon dioxide. Nano Research, 2019, 12, 1167-1172.	10.4	41
49	Converting Metal–Organic Framework Particles from Hydrophilic to Hydrophobic by an Interfacial Assembling Route. Langmuir, 2017, 33, 12427-12433.	3.5	39
50	Metal–Organic Framework-Stabilized CO <sub>2</sub> /Water Interfacial Route for Photocatalytic CO <sub>2</sub> Conversion. ACS Applied Materials & Interfaces, 2017, 9, 41594-41598.	8.0	39
51	Boron-doped CuO nanobundles for electroreduction of carbon dioxide to ethylene. Green Chemistry, 2020, 22, 2750-2754.	9.0	39
52	Preparation of ZnS/CdS composite nanoparticles by coprecipitation from reverse micelles using CO2 as antisolvent. Journal of Colloid and Interface Science, 2004, 273, 160-164.	9.4	38
53	High internal ionic liquid phase emulsion stabilized by metal–organic frameworks. Soft Matter, 2016, 12, 8841-8846.	2.7	38
54	Roomâ€Temperature Synthesis of Covalent Organic Framework (COF‣ZU1) Nanobars in CO <sub>2</sub> /Water Solvent. ChemSusChem, 2018, 11, 3576-3580.	6.8	38

#	Article	IF	CITATIONS
55	Macro―and Mesoporous Polymers Synthesized by a CO <sub>2</sub> â€inâ€ionic Liquid Emulsionâ€Templating Route. Angewandte Chemie - International Edition, 2013, 52, 1792-1795.	13.8	37
56	A Pd–Cu <sub>2</sub> O nanocomposite as an effective synergistic catalyst for selective senergistic catalyst for selective semi-hydrogenation of the terminal alkynes only. Chemical Communications, 2016, 52, 3627-3630.	4.1	37
57	Highly Mesoporous Ru-MIL-125-NH <sub>2</sub> Produced by Supercritical Fluid for Efficient Photocatalytic Hydrogen Production. ACS Applied Energy Materials, 2019, 2, 4964-4970.	5.1	37
58	Supercritical CO2 produces the visible-light-responsive TiO2/COF heterojunction with enhanced electron-hole separation for high-performance hydrogen evolution. Nano Research, 2020, 13, 983-988.	10.4	37
59	Ultra-small gold nanoparticles immobilized on mesoporous silica/graphene oxide as highly active and stable heterogeneous catalysts. Chemical Communications, 2015, 51, 4398-4401.	4.1	36
60	Metal–Organic Framework for Emulsifying Carbon Dioxide and Water. Angewandte Chemie - International Edition, 2016, 55, 11372-11376.	13.8	36
61	A Novel Method to Synthesize Polystyrene Nanospheres Immobilized with Silver Nanoparticles by Using Compressed CO2. Chemistry - A European Journal, 2004, 10, 3531-3536.	3.3	34
62	Nanosized Poly(ethylene glycol) Domains within Reverse Micelles Formed in CO <sub>2</sub> . Angewandte Chemie - International Edition, 2012, 51, 12325-12329.	13.8	32
63	Mesoporous inorganic salts with crystal defects: unusual catalysts and catalyst supports. Chemical Science, 2015, 6, 1668-1675.	7.4	32
64	Cu <sub>x</sub> Ni <sub>y</sub> alloy nanoparticles embedded in a nitrogen–carbon network for efficient conversion of carbon dioxide. Chemical Science, 2019, 10, 4491-4496.	7.4	32
65	Simultaneous CO <sub>2</sub> Reduction and 5-Hydroxymethylfurfural Oxidation to Value-Added Products by Electrocatalysis. ACS Sustainable Chemistry and Engineering, 2022, 10, 8043-8050.	6.7	32
66	Reversible Switching of Lamellar Liquid Crystals into Micellar Solutions using CO <sub>2</sub> . Angewandte Chemie - International Edition, 2008, 47, 10119-10123.	13.8	31
67	Flexible superhydrophobic polysiloxane aerogels for oil–water separation via one-pot synthesis in supercritical CO <sub>2</sub> . RSC Advances, 2015, 5, 76346-76351.	3.6	31
68	Synthesis of icosahedral gold particles by a simple and mild route. Green Chemistry, 2008, 10, 1094.	9.0	29
69	Improved catalytic performance of Co-MOF-74 by nanostructure construction. Green Chemistry, 2020, 22, 5995-6000.	9.0	29
70	Improved photocatalytic performance of covalent organic frameworks by nanostructure construction. Chemical Communications, 2020, 56, 4567-4570.	4.1	29
71	Gas promotes the crystallization of nano-sized metal–organic frameworks in ionic liquid. Chemical Communications, 2015, 51, 11445-11448.	4.1	28
72	<i>In situ</i> synthesis of sub-nanometer metal particles on hierarchically porous metal–organic frameworks <i>via</i> interfacial control for highly efficient catalysis. Chemical Science, 2018, 9, 1339-1343.	7.4	28

#	Article	IF	CITATIONS
73	An NH <sub>2</sub> -MIL-125 (Ti)/Pt/g-C <sub>3</sub> N <sub>4</sub> catalyst promoting visible-light photocatalytic H <sub>2</sub> production. Sustainable Energy and Fuels, 2019, 3, 1233-1238.	4.9	27
74	Fabrication of NH <sub>2</sub> -MIL-125 nanocrystals for high performance photocatalytic oxidation. Sustainable Energy and Fuels, 2020, 4, 2823-2830.	4.9	27
75	Preparation of cadmium sulfide/poly(methyl methacrylate) composites by precipitation with compressed CO2. Journal of Applied Polymer Science, 2004, 94, 1643-1648.	2.6	26
76	Metal Ionic Liquids for the Rapid Chemical Fixation of CO <sub>2</sub> under Ambient Conditions. ChemCatChem, 2020, 12, 1963-1967.	3.7	25
77	Formation of multiple water-in-ionic liquid-in-water emulsions. Journal of Colloid and Interface Science, 2012, 368, 395-399.	9.4	24
78	Room-temperature synthesis of mesoporous CuO and its catalytic activity for cyclohexene oxidation. RSC Advances, 2015, 5, 67168-67174.	3.6	24
79	Amphiphile self-assemblies in supercritical CO <sub>2</sub> and ionic liquids. Soft Matter, 2014, 10, 5861-5868.	2.7	23
80	lonic liquids produce heteroatom-doped Pt/TiO2 nanocrystals for efficient photocatalytic hydrogen production. Nano Research, 2019, 12, 1967-1972.	10.4	23
81	Effect of compressed CO2 on the properties of AOT reverse micelles studied by spectroscopy and phase behavior. Journal of Chemical Physics, 2003, 119, 4873-4878.	3.0	21
82	Switching Micellization of Pluronics in Water by CO <sub>2</sub> . Chemistry - A European Journal, 2011, 17, 4266-4272.	3.3	21
83	Improved photocatalytic performance of metal–organic frameworks for CO <sub>2</sub> conversion by ligand modification. Chemical Communications, 2020, 56, 7637-7640.	4.1	21
84	Enhancing CO <sub>2</sub> electroreduction to CH <sub>4</sub> over Cu nanoparticles supported on N-doped carbon. Chemical Science, 2022, 13, 8388-8394.	7.4	21
85	Effect of compressed CO2 on the size and stability of reverse micelles: Small-angle x-ray scattering and phase behavior study. Journal of Chemical Physics, 2003, 118, 3329-3333.	3.0	19
86	Steering CO2 electroreduction toward methane or ethylene production. Nano Energy, 2021, 88, 106239.	16.0	19
87	Photocatalytic carbon dioxide reduction coupled with benzylamine oxidation over Zn-Bi <sub>2</sub> WO <sub>6</sub> microflowers. Green Chemistry, 2021, 23, 2913-2917.	9.0	19
88	A new separation method: combination of CO2 and surfactant aqueous solutions. Green Chemistry, 2008, 10, 578.	9.0	18
89	Waterâ€inâ€Supercritical CO <sub>2</sub> Microemulsion Stabilized by a Metal Complex. Angewandte Chemie - International Edition, 2016, 55, 13533-13537.	13.8	18
90	Highly selective and efficient reduction of CO <sub>2</sub> to CO on cadmium electrodes derived from cadmium hydroxide. Chemical Communications, 2018, 54, 5450-5453.	4.1	18

#	Article	IF	CITATIONS
91	Synthesis of montmorillonite/polystyrene nanocomposites in supercritical carbon dioxide. Journal of Applied Polymer Science, 2004, 94, 1194-1197.	2.6	17
92	Effects of ultrasound on the microenvironment in reverse micelles and synthesis of nanorods and nanofibers. Physical Chemistry Chemical Physics, 2004, 6, 2391.	2.8	17
93	Preparation of mesoporous MCM-41/poly(acrylic acid) composites using supercritical CO2 as a solvent. Journal of Materials Chemistry, 2003, 13, 1373.	6.7	16
94	Porosity control in mesoporous polymers using CO <sub>2</sub> -swollen block copolymer micelles as templates and their use as catalyst supports. Chemical Communications, 2014, 50, 11957-11960.	4.1	16
95	Assembly of Mesoporous Metal–Organic Framework Templated by an Ionic Liquid/Ethylene Glycol Interface. ChemPhysChem, 2015, 16, 2317-2321.	2.1	16
96	Solvent Impedes CO <sub>2</sub> Cycloaddition on Metal–Organic Frameworks. Chemistry - an Asian Journal, 2018, 13, 386-389.	3.3	16
97	Rapid, Roomâ€Temperature and Templateâ€Free Synthesis of Metalâ€Organic Framework Nanowires in Alcohol. ChemCatChem, 2019, 11, 2058-2062.	3.7	16
98	Boosting CO <sub>2</sub> electroreduction to C <sub>2+</sub> products on fluorine-doped copper. Green Chemistry, 2022, 24, 1989-1994.	9.0	16
99	Synthesis of Ag/BSA composite nanospheres from water-in-oil microemulsion using compressed CO2 as antisolvent. Biotechnology and Bioengineering, 2005, 89, 274-279.	3.3	14
100	CO2-responsive TX-100 emulsion for selective synthesis of 1D or 3D gold. Soft Matter, 2010, 6, 6200.	2.7	14
101	Emulsion inversion induced by CO2. Physical Chemistry Chemical Physics, 2011, 13, 6065.	2.8	14
102	A simple and inexpensive route to synthesize porous silica microflowers by supercritical CO2. Microporous and Mesoporous Materials, 2005, 87, 10-14.	4.4	13
103	CO2-controlled reactors: epoxidation in emulsions with droplet size from micron to nanometre scale. Green Chemistry, 2010, 12, 452.	9.0	13
104	Hierarchically macro–meso–microporous metal–organic framework for photocatalytic oxidation. Chemical Communications, 2020, 56, 10754-10757.	4.1	13
105	Air atmospheric photocatalytic oxidation by ultrathin C,N-TiO <sub>2</sub> nanosheets. Green Chemistry, 2021, 23, 1165-1170.	9.0	13
106	Template-free synthesis of mesoporous polymers. Chemical Communications, 2014, 50, 8128-8130.	4.1	12
107	Switching chirality in the assemblies of bio-based amphiphiles solely by varying their alkyl chain length. Chemical Communications, 2017, 53, 2162-2165.	4.1	12
108	Pickering emulsions stabilized by metal–organic frameworks, graphitic carbon nitride and graphene oxide. Soft Matter, 2021, 18, 10-18.	2.7	12

#	Article	IF	CITATIONS
109	Tin(IV) Sulfide Greatly Improves the Catalytic Performance of UiOâ€66 for Carbon Dioxide Cycloaddition. ChemCatChem, 2018, 10, 2945-2948.	3.7	11
110	CO <sub>2</sub> /Water Emulsions Stabilized by Partially Reduced Graphene Oxide. ACS Applied Materials & Interfaces, 2017, 9, 17613-17619.	8.0	10
111	Efficient separation of surfactant and organic solvent by CO2. Chemical Communications, 2011, 47, 5816.	4.1	9
112	Interfacial assembly and hydrolysis for synthesizing a TiO2/metal–organic framework composite. Soft Matter, 2017, 13, 9174-9178.	2.7	9
113	Carbon dioxide droplets stabilized by g-C <sub>3</sub> N <sub>4</sub> . Green Chemistry, 2018, 20, 4206-4209.	9.0	9
114	Ferric acetylacetonate/covalent organic framework composite for high performance photocatalytic oxidation. Green Energy and Environment, 2022, 7, 1281-1288.	8.7	9
115	Preparation of high entropy nitride ceramic nanofibers from liquid precursor for CO <sub>2</sub> photocatalytic reduction. Journal of the American Ceramic Society, 2022, 105, 3729-3734.	3.8	9
116	Metal–Organic Framework for Emulsifying Carbon Dioxide and Water. Angewandte Chemie, 2016, 128, 11544-11548.	2.0	8
117	Ultra-small UiO-66-NH2 nanoparticles immobilized on g-C3N4 nanosheets for enhanced catalytic activity. Green Energy and Environment, 2022, 7, 512-518.	8.7	8
118	Water nanodomains for efficient photocatalytic CO <sub>2</sub> reduction to CO. Green Chemistry, 2021, 23, 9078-9083.	9.0	8
119	Ultrasound-Induced Capping of Polystyrene on TiO <sub>2</sub> Nanoparticles by Precipitation with Compressed CO <sub>2</sub> as Antisolvent. Journal of Nanoscience and Nanotechnology, 2005, 5, 945-950.	0.9	7
120	Enhanced stabilization of vesicles formed in mixed cationic and anionic surfactant systems by compressed gases. RSC Advances, 2011, 1, 776.	3.6	7
121	Waterâ€inâ€5upercritical CO <sub>2</sub> Microemulsion Stabilized by a Metal Complex. Angewandte Chemie, 2016, 128, 13731-13735.	2.0	6
122	Formation of large nanodomains in liquid solutions near the phase boundary. Chemical Communications, 2016, 52, 14286-14289.	4.1	6
123	Metal Ionic Liquids Produce Metalâ€Dispersed Carbonâ€Nitrogen Networks for Efficient CO 2 Electroreduction. ChemCatChem, 2019, 11, 3166-3170.	3.7	6
124	BiO <sub>2-x</sub> Nanosheets with Surface Electron Localizations for Efficient Electrocatalytic CO <sub>2</sub> Reduction to Formate. CCS Chemistry, 2023, 5, 133-144.	7.8	6
125	Co(NO <sub>3</sub> ) <sub>2</sub> /covalent organic framework nanoparticles for high-efficiency photocatalytic oxidation of thioanisole. Chemical Communications, 2022, 58, 6324-6327.	4.1	5
126	Anchoring Ionic Liquid in Copper Electrocatalyst for Improving CO <sub>2</sub> Conversion to Ethylene. Angewandte Chemie, 2022, 134, .	2.0	4

#	Article	IF	CITATIONS
127	Periodically nanoporous hydrogen-bonded organic frameworks for high performance photocatalysis. Nanoscale, 2022, 14, 9762-9770.	5.6	4
128	Ultrathin and Porous Carbon Nanosheets Supporting Bimetallic Nanoparticles for Highâ€Performance Electrocatalysis. ChemCatChem, 2018, 10, 1241-1247.	3.7	3
129	Effect of ultrasound on the microstructure of polystyrene in cyclohexane: a synchrotron small-angle X-ray scattering study. Colloid and Polymer Science, 2007, 285, 1275-1279.	2.1	2
130	CO2as a smart gelator for Pluronic aqueous solutions. Chemical Communications, 2014, 50, 14233-14236.	4.1	2
131	Hierarchical macro- and mesoporous assembly of metal oxide nanoparticles derived from metal-organic complex. Microporous and Mesoporous Materials, 2015, 217, 6-11.	4.4	2
132	Highly Crystalline Agâ€based Coordination Polymers for Efficient Photocatalytic Oxidation of Sulfides. Chemistry - an Asian Journal, 2022, , e202200031.	3.3	2
133	Water–alkane interface promotes the formation of metal–organic frameworks. Microporous and Mesoporous Materials, 2016, 220, 270-274.	4.4	1
134	The stability of metal-organic framework MIL-101(Fe) in alkylol amine solutions. Scientia Sinica Chimica, 2022, , .	0.4	0
135	Two highly crystalline coordination polymers with two-dimensional PbS networks for photocatalytic synthesis of imines. Catalysis Science and Technology, 0, , .	4.1	0